2010-05-01

Analysis of apoptosis of memory T cells and dendritic cells during the early stages of viral infection or exposure to toll-like receptor agonists

Kapil Bahl
Yale University

Et al.

JOURNAL OF VIROLOGY, May 2010, p. 4866–4877 Vol. 84, No. 10
0022-538X/10/$12.00 doi:10.1128/JVI.02571-09

Analysis of Apoptosis of Memory T Cells and Dendritic Cells during the Early Stages of Viral Infection or Exposure to Toll-Like Receptor Agonists▽

Kapil Bahl,[1] Anette Hüebner,[3] Roger J. Davis,[3] and Raymond M. Welsh[2]*

Department of Pathology, Yale University School of Medicine, New Haven, Connecticut 06510[1]; Department of Pathology, Program in Immunology and Virology, University of Massachusetts Medical School, Worcester, Massachusetts 01655[2]; and Howard Hughes Medical Institute, University of Massachusetts Medical School, Worcester, Massachusetts 01605[3]

Received 8 December 2009/Accepted 23 February 2010

Profound type I interferon (IFN-I)-dependent attrition of memory CD8 and CD4 T cells occurs early during many infections. It is dramatic at 2 to 4 days following lymphocytic choriomeningitis virus (LCMV) infection of mice and can be elicited by the IFN-inducing Toll receptor agonist poly(I:C). We show that this attrition occurs in many organs, indicating that it is due to T cell loss rather than redistribution. This loss correlated with elevated intracellular staining of T cells *ex vivo* for activated caspases but with only low levels of *ex vivo* staining with annexin V, probably due to the rapid clearance of apoptotic cells *in vivo*. Instead, a high frequency of annexin V-reactive CD8α$^+$ dendritic cells (DCs), which are known to be highly phagocytic, accumulated in the spleen as the memory T cell populations disappeared. After short *in vitro* incubation, memory phenotype T cells isolated from LCMV-infected mice (day 3) or mice treated with poly(I:C) (12 h) displayed substantial DNA fragmentation, as detected by terminal deoxynucleotidyltransferase-mediated dUTP-biotin nick end labeling (TUNEL) assay, compared to T cells isolated from uninfected mice, indicating a role for apoptosis in the memory T cell attrition. This apoptosis of memory CD8 T cells early during LCMV infection was reduced in mice lacking the proapoptotic molecule Bim. Evidence is presented showing that high levels of T cell attrition, as found in young mice, correlate with reduced immunodomination by cross-reactive memory cells.

A pronounced type I interferon (IFN-I)-dependent, body-wide attrition of "memory phenotype" (CD44^{high}) CD8$^+$ T cells occurs in mice during the early stages of viral infections or after exposure to IFN-I-inducing toll-like receptor (TLR) agonists, such as poly(I:C) (3, 27). This attrition can also be induced by injection of mice with IFN-I and is not seen in virus-infected or TLR agonist-treated mice lacking IFN-I receptors (27). Severe attrition of T cells can be seen in other animal models (31, 35), and a severe lymphopenia is a common pathological characteristic of human infections with many viruses, including measles virus, influenza virus, Ebola virus, Lassa fever virus, lymphocytic choriomeningitis virus (LCMV), West Nile virus, and severe acute respiratory syndrome (SARS) virus (3, 4, 13, 14, 27, 30, 33, 45). The disappearance of memory T cells from the blood can be due to other factors, such as the IFN-I-driven sequestration of T cells in lymph nodes, so in many of the human studies there has not been a body-wide analysis of T cell loss. Here we are referring to a global attrition throughout the body in these mouse studies.

The mechanisms behind this global T cell attrition in mice remain poorly understood and could be associated with different pathways, including direct killing of T cells by a virus (unlikely with LCMV), migration of T cells to sites inaccessible for analysis, or cytokine-driven apoptosis of memory T cells. IFN-I dependence of memory cell loss was originally shown in mice at 2 to 4 days after LCMV infection (27). This early attrition was characterized by losses in many types of leukocytes, but *bona fide* antigen-specific memory cells and memory phenotype CD8$^+$ CD44^{high} T cells were among the most susceptible. This loss in memory CD8 T cells has also been shown with the TLR agonist and potent IFN-I inducer poly(I:C), and this attrition has been thought to be due to apoptosis, since CD8α$^+$ CD44^{high} cells stain positively with active caspase substrates and with the early apoptosis marker annexin V (3, 21, 27). Our continued analyses of these systems showed a similar attrition of CD44^{high} CD4 T cells, but this population did not costain highly with annexin V directly *ex vivo*. This led us to question if the losses of CD8$^+$ CD44^{high} and CD4$^+$ CD44^{high} T cells were occurring by different mechanisms.

Here we show that the increased annexin V$^+$ CD8α$^+$ CD44^{high} population consisted mostly of highly phagocytic lymphoid-like CD8α$^+$ dendritic cells (DCs) instead of T cells. At these early stages after poly(I:C) induction or viral infection, the number of CD8α$^+$ DCs increases substantially, and the phagocytic clearance system appears to be so efficient that most *bona fide* dying T cells are likely cleared before they can be stained for annexin V or DNA fragmentation (terminal deoxynucleotidyltransferase-mediated dUTP-biotin nick end labeling [TUNEL]) immediately *ex vivo*. This is not true later on in infection, when annexin V-positive (annexin V$^+$) *bona fide* antigen-specific CD8 T

* Corresponding author. Mailing address: Department of Pathology, Program in Immunology and Virology, University of Massachusetts Medical School, 55 Lake Avenue North, Worcester, MA 01655. Phone: (508) 856-2008. Fax: (508) 856-1095. E-mail: Raymond.Welsh@umassmed.edu.

▽ Published ahead of print on 3 March 2010.

cells can easily be detected, as the clearance system for dying cells seems to be overwhelmed (40, 41).

At early stages of infection, the annexin V-reactive CD8α$^+$ cells were therefore predominantly DCs and not T cells. This caused us to undertake a further analysis of the mechanism of attrition of the CD8$^+$ CD44^{high} and CD4$^+$ CD44^{high} T cell populations. We show here that virus- and poly(I:C)-induced IFN-I-mediated apoptosis of CD8$^+$ CD44^{high} and CD4$^+$ CD44^{high} T cells does indeed occur, but this requires a short *in vitro* incubation to demonstrate the DNA fragmentation. Furthermore, the loss of CD8α$^+$ CD44^{high} T cells was even greater than previously thought, due to the contamination with the CD8α$^+$ DC population, which bound to annexin V. Further, we show that the IFN-I-induced apoptosis of these memory T cells is impaired in mice lacking the proapoptotic protein Bim.

MATERIALS AND METHODS

Virus stocks. LCMV strain Armstrong, an ambisense RNA virus in the Old World arenavirus family, and Pichinde virus (PV), strain AN3739, a New World arenavirus only distantly related to LCMV, were propagated in BHK21 baby hamster kidney cells (42, 46). LCMV and PV were titrated by plaque assay on Vero cells.

Mice. Male C57BL/6 mice were purchased from The Jackson Laboratory (Bar Harbor, ME). All mice were purchased at 5 to 6 weeks of age and maintained under specific-pathogen-free conditions within the Department of Animal Medicine at the University of Massachusetts Medical School. C57BL/6-Bim knockout mice (Bim KO) were originally generated by Andreas Strasser (6) and were purchased from the Jackson Laboratory. Mice were infected intraperitoneally (i.p.) with 5×10^4 PFU of LCMV and were considered immune at 6 weeks or longer after infection. All experiments were done within institutional guidelines as approved by the Institutional Animal Care and Use Committee of the University of Massachusetts Medical School.

Lymphocyte preparation for flow cytometric analysis. Spleens and inguinal lymph nodes (iLN) were isolated from tissue and homogenized using frosted glass slides. Lungs were isolated from the tissue and cut into small pieces with razor blades, followed by further homogenization using frosted glass slides. The resulting cell suspensions from all three organs were depleted of red blood cells using a 0.84% NH_4Cl solution (5 min at 4°C). For the isolation of peritoneal exudate cells (PECs), the skin was removed while leaving the peritoneal membrane intact. Approximately 6 ml of cold RPMI was injected into the peritoneal cavity using an 18-gauge needle and then aspirated to collect PECs. Peripheral blood lymphocytes (PBLs) were isolated via tail vein bleeding, and red blood cells were depleted using a 0.84% NH_4Cl solution (10 min at 37°C). All cell suspensions were washed in phosphate-buffered saline (PBS) and filtered through nylon mesh prior to flow cytometry staining.

Apoptosis assays. For some experiments, apoptosis was evaluated via flow cytometry using fluorescently conjugated annexin V (BD Pharmingen). Upon the completion of surface staining, the cells were washed and incubated in annexin V binding buffer with annexin V at a 1:20 dilution for 15 min at room temperature. The cells were then washed, resuspended in annexin V binding buffer, and analyzed by flow cytometry immediately. Annexin V staining was done in conjunction with the vital dye 7-amino-actinomycin D (7-AAD) to differentiate early apoptosis (annexin V$^+$ 7-AAD$^-$) from late apoptosis/necrosis (annexin V$^+$ 7-AAD$^+$).

Apoptosis was also evaluated via flow cytometry using terminal deoxynucleotidyltransferase-mediated dUTP-biotin nick end labeling (TUNEL). Erythrocytes were removed from harvested splenocytes using a 0.84% NH_4Cl solution. Spleen leukocytes were added to a 48-well plate at 1×10^6 cells per well and incubated at either 37°C (5% CO_2) or 4°C for 5 h. Cells were then harvested and stained with the appropriate fluorescent surface antibodies. Upon completion of surface staining, the cells were fixed according to the manufacturer's protocol. TUNEL-positive (TUNEL$^+$) cells were detected using an ApoDIRECT in situ DNA fragmentation assay kit (BioVision).

Synthetic peptides. Previously defined T cell epitopes encoded by LCMV were used in this study (36, 43). LCMV-specific epitopes include GP33-41 (KAVYN FATC) and NP205-212 (YTVKYPNL). A previously defined T cell epitope encoded by PV, NP38-45 (SALDFHKV), was also used in this study (8). All peptides listed above were purchased from 21st Century Biochemicals and were purified by reverse-phase high-pressure liquid chromatography (HPLC) to 90% purity.

Inoculations. Poly(I:C) (Invivogen) was administered at a dose of 200 μg in 200 μl of Hanks balanced salt solution (HBSS) per mouse i.p. For the induction of an acute LCMV-Armstrong infection, mice were injected i.p. with 5×10^4 PFU of virus in 0.1 ml of PBS. For the induction of an acute PV infection, mice were injected i.p. with 2×10^7 PFU of virus in 0.1 ml of PBS.

Intracellular IFN-γ staining. LCMV-specific memory CD8 T cells were detected by measuring intracellular IFN-γ production in response to stimulation with LCMV peptides using the Cytofix/Cytoperm Kit Plus (with GolgiPlug; BD Pharmingen), as described previously (38). Spleen leukocytes (2×10^6) were incubated in 96-well plates (5 h; 37°C) with 1 μM synthetic peptide, 10 U/ml human recombinant interleukin-2 (rIL-2) (BD Pharmingen) and 0.2 μl of GolgiPlug (BD Pharmingen). Cells were then washed in flow cytometry buffer (HBBS, 2% fetal calf serum [FCS], and 0.1% NaN_3), blocked with anti-Fc (2.4G2), and incubated (30 min; 4°C) with the appropriate fluorescent surface antibodies (BD Pharmingen and eBioscience). Subsequent fixation and permeabilization of the cells were performed to allow intracellular access of monoclonal antibody (MAb) to IFN-γ and tumor necrosis factor (TNF) (eBioscience). Freshly stained samples were analyzed on a BD Biosciences LSR II with FlowJo software.

Statistical analyses. Student's *t* test and linear correlation were calculated using GraphPad InStat and used for data analysis where appropriate. Results are expressed as the mean ± standard deviation.

RESULTS

Poly(I:C)-induced attrition of T cells does not correlate with an increase in annexin V reactivity on T cells. We initially reevaluated the attrition of CD8 and CD4 T cells in mice stimulated with the type I IFN inducer poly(I:C). Figure 1 shows that poly(I:C) treatment of C57BL/6 mice resulted in a 52% decrease in the percentage of CD8α$^+$ CD44^{high} cells relative to the untreated control (Fig. 1A) and a corresponding 2.5-fold increase in the percentage of annexin V reactivity at 12 h postinoculation (Fig. 1B). CD4$^+$ CD44^{high} cells underwent a similar loss in percentage (58%) (Fig. 1A) but, surprisingly, did not have a substantial increase in annexin V reactivity after poly(I:C) inoculation (Fig. 1B). We questioned why the annexin V staining of these two disappearing populations differed, so we utilized a MAb to the CD8β chain to further define the CD8 cell population. There was a higher (71%) decrease in the percentage of CD8β$^+$ CD44^{high} cells than of CD8α$^+$ CD44^{high} cells following poly(I:C) treatment (Fig. 1A), but this population, like the CD4 cells, had no corresponding increase in annexin V reactivity (Fig. 1B). No increase in annexin V reactivity was observed in any of the three CD44^{low} populations following poly(I:C) treatment (data not shown).

These data suggested that there was an increased population of annexin V-reactive cells expressing a CD8α homodimer (CD8αα$^+$) and lacking CD8β, so we further characterized this population of CD8αα$^+$ cells. An apoptosis RT^2 Profiler PCR array revealed an 11-fold increase in CD40 RNA isolated from CD8α$^+$ CD44^{high} cells at 6 h after poly(I:C) relative to an untreated control (data not shown). Typically, CD40 surface protein expression is thought to be limited to B cells, DCs, and macrophages (5), although CD8 T cells, under certain conditions, may transiently express CD40 (7). There was a substantial increase in CD40 protein on the surface of the CD8α$^+$ CD44^{high} population at 12 h after poly(I:C) treatment, relative to the untreated control (Fig. 1C), and this increase in CD40 expression directly correlated with an increase in annexin V reactivity (Fig. 1D). In contrast, CD40 surface protein expression was low on the

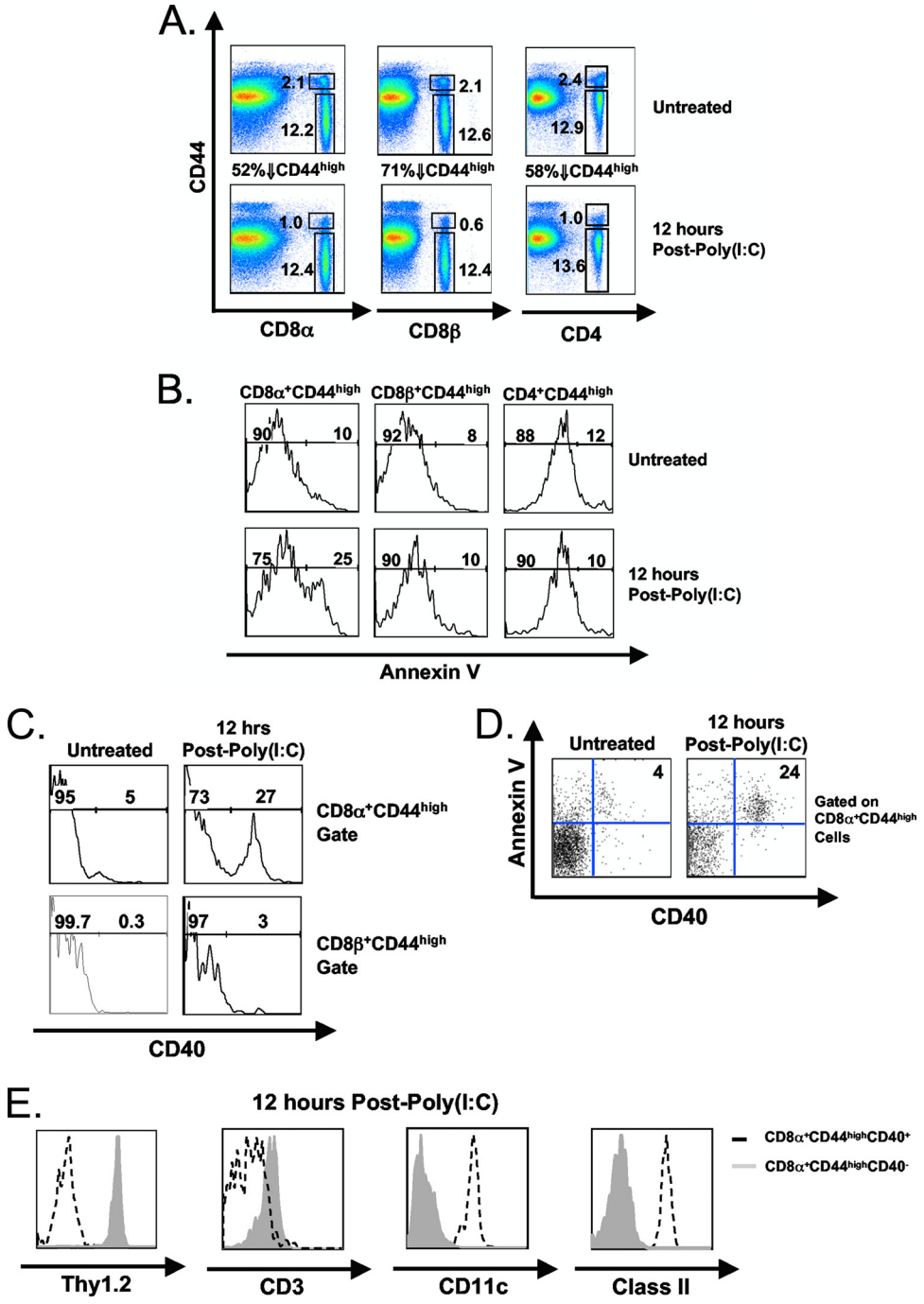

FIG. 1. An increase in CD8α$^+$ DCs accounts for the observed increase in annexin V-reactive CD8α$^+$ CD44^{high} cells following poly(I:C) treatment. C57BL/6 mice were inoculated with poly(I:C) i.p. Splenocytes were harvested at 0 h (untreated) and 12 h postinoculation. (A) Percentages of untreated and poly(I:C)-treated CD8α$^+$ CD44$^{high/low}$, CD8β$^+$ CD44$^{high/low}$, and CD4$^+$ CD44$^{high/low}$ cells. (B) Percentages of untreated and poly(I:C)-treated annexin V$^+$ CD8α$^+$ CD44^{high}, annexin V$^+$ CD8β$^+$ CD44^{high}, and annexin V$^+$ CD4$^+$ CD44^{high} cells. (C) CD40 expression on untreated or poly(I:C)-treated CD8α$^+$ CD44^{high} and CD8β$^+$ CD44^{high} cells. (D) Annexin V and CD40 expression on untreated or poly(I:C)-treated CD8α$^+$ CD44^{high} cells. (E) Thy1.2, CD3, CD11c, and class II (I-A^B) expression on untreated or poly(I:C)-treated CD40$^+$ CD8α$^+$ CD44^{high} (dashed lines) and CD40$^-$ CD8α$^+$ CD44^{high} (gray fill) cells. Gates were set upon 7-AAD$^-$ cells to exclude dead/necrotic cells. The data are representative of three independent experiments with three mice per group.

CD8β$^+$ CD44^{high} population following poly(I:C) treatment (3%) (Fig. 1C). Since CD40 expression directly correlated with an increase in annexin V reactivity, we questioned whether CD40 expression was necessary for the poly(I:C)-induced attrition. Both wild-type and CD40 KO mice, however, showed a similar decrease in CD8α$^+$ CD44^{high} cells along with a similar corresponding increase in annexin V reactivity following poly(I:C) treatment (data not shown).

This suggested that the poly(I:C)-induced attrition of $CD8\alpha^+$ $CD44^{high}$ cells was not dependent on the expression of CD40.

We next used a MAb to the pan T cell marker Thy 1.2 to further characterize these cell populations. While the $CD40^-$ $CD8\alpha^+$ $CD44^{high}$ population expressed Thy1.2, the $CD40^+$ $CD8\alpha^+$ $CD44^{high}$ population did not (Fig. 1E), indicating that this population did not consist of T cells. This was further confirmed using a MAb to T cell receptor-associated CD3 (Fig. 1E). We then questioned whether this population of $CD40^+$ $CD8\alpha^+$ $CD44^{high}$ cells was a subset of DCs, since certain DC populations can express $CD8\alpha\alpha^+$ (29, 39). This cell population strongly expressed both CD11c and major histocompatibility complex (MHC) class II, consistent with a DC phenotype (Fig. 1E), and failed to stain with the B cell marker B220 (data not shown). Collectively, these results show that this population displays a "lymphoid" DC phenotype that greatly accumulates in the spleen rapidly after poly(I:C) treatment.

Kinetic analysis of the poly(I:C)-induced increase in $CD8\alpha^+$ DCs revealed a 2-fold increase in the percentage of $CD8\alpha^+$ DCs in the spleen as early as 9 h and a 3-fold increase by 12 h after poly(I:C) treatment, relative to the untreated control (Fig. 2A). This increase in percentage corresponded to a 2-fold increase in total $CD8\alpha^+$ DC number at 9 and 12 h after poly(I:C) treatment (Fig. 2B). This poly(I:C)-induced increase in splenic $CD8\alpha^+$ DC number coupled with the decrease in $CD8\alpha^+$ $CD44^{high}$ T cell number was such that the $CD8\alpha^+$ DC population became a substantial fraction of the $CD8\alpha^+$ $CD44^{high}$ cells. This means that the poly(I:C)-induced loss of $CD8^+$ $CD44^{high}$ T cells had actually been underestimated. Furthermore, the observed increase in annexin V^+ cells was due to reactivity with the increasing $CD8\alpha^+$ DC population rather than the reduced T cell population. The fact that this early T cell attrition did not correlate with an increase in T cell annexin V reactivity left it unclear as to whether the T cell attrition was indeed due to apoptosis.

The attrition of T cells correlates with an increase in DNA fragmentation. In light of these findings, it was necessary to reevaluate the early attrition of $CD8^+$ T cells using an anti-CD8β antibody, which is a more exclusive marker for $CD8^+$ T cells than an anti-CD8α antibody. We first conducted a kinetic analysis of the poly(I:C)-induced attrition of $CD8\beta^+$ $CD44^{high}$ T cells in the spleen. This time course study revealed a 27% decrease in the percentage of $CD8\beta^+$ $CD44^{high}$ T cells as early as 3 h after poly(I:C) treatment and a 51% decline at 12 h, relative to untreated controls (Fig. 2C). This was reflected in a statistically significant decrease in $CD8\beta^+$ $CD44^{high}$ T cell number at 12 h after poly(I:C) treatment, relative to the untreated control (Fig. 2D). Figure 2B shows the concomitant increase in splenic $CD8\alpha^+$ DC number in the same animals. This reduction in splenic $CD8\beta^+$ $CD44^{high}$ T cells could not be explained by trafficking to other organs, as the PECs, lungs, iLN, and peripheral blood all exhibited significant, although varying, decreases in the percentage of $CD8\beta^+$ $CD44^{high}$ T cells at 12 h following poly(I:C) treatment (Fig. 3A). The attrition of $CD4^+$ $CD44^{high}$ T cells also occurred in all organs tested following poly(I:C) treatment (Fig. 3B). The percentages of $CD8\alpha^+$ DCs in the PECs, lungs, iLN, and peripheral blood were substantially lower (<0.1%) than those in the spleen, and there was no increase observed in these organs following poly(I:C) treatment (data not shown). These data support the notion that the IFN-I-induced attrition of T cells was a "global" phenomenon and could not be explained by migration out of the spleen, although a small redistribution of cells cannot be completely ruled out.

We next questioned whether the poly(I:C)-induced loss of T cells was due to apoptosis and used the TUNEL assay to measure DNA fragmentation as an unambiguous indicator of apoptotic cells. As commonly found by us and others, detection of $TUNEL^+$ cells *in vivo* was difficult, as dying cells are rapidly scavenged by phagocytic cells bearing receptors for phosphatidylserine, which is expressed on the surface of apoptotic cells (37). Therefore, splenocytes isolated from either untreated or poly(I:C)-treated wild-type mice were incubated at 37°C for 5 h *in vitro*. This technique has been shown in other studies to reveal DNA fragmentation in freshly isolated cells *ex vivo* (40, 41). As a control, splenocytes were also incubated at 4°C for 5 h. Incubation at this nonphysiological temperature should inhibit DNA fragmentation, since metabolic processes would be hindered. After a brief incubation at 37°C, there was an increase in the percentage of $TUNEL^+$ $CD8\beta^+$ $CD44^{high}$ T cells following poly(I:C) treatment, relative to the untreated controls ($n = 3$; $P < 0.02$) (Fig. 4A). Although the background levels of TUNEL staining were higher for $CD4^+$ $CD44^{high}$ T cells, they showed a trend similar to that for $CD8\beta^+$ $CD44^{high}$ T cells ($n = 3$; $P < 0.01$) (Fig. 4B). These results indicate that at least some of the attrition of both $CD8\beta^+$ $CD44^{high}$ and $CD4^+$ $CD44^{high}$ T cell populations, following poly(I:C) treatment, occurs through an apoptotic mechanism.

$CD8\alpha^+$ DCs may aid in the clearance of apoptotic cells following poly(I:C) treatment. It has been shown that the "lymphoid" $CD8\alpha^+$ DC population, similar to that shown to increase in our system, is capable of phagocytosing apoptotic cells (1, 2) and that monocytes that phagocytose apoptotic bodies from neighboring apoptotic cells become "false positive" and react with annexin V (25). This suggests that $CD8\alpha^+$ DCs might also become annexin V^+ upon engulfing apoptotic lymphocytes. Therefore, we examined whether this $CD8\alpha^+$ DC population might be involved in the clearance of apoptotic cells following poly(I:C) treatment. To do this, we adoptively transferred carboxyfluorescein succinimidyl ester (CFSE)-labeled wild-type spleen leukocytes (Ly5.1) into congenic wild-type hosts (Ly5.2) and harvested splenocytes at multiple time points following poly(I:C) treatment. The $Ly5.2^+$ $CD8\alpha^+$ $CD11c^+$ DC population assimilated CFSE at 9 and 12 h after poly(I:C) treatment, correlating with an increase in their expression of the activation marker CD40, while the $Ly5.2^+$ $CD8\alpha^-$ $CD11c^+$ DC population had a relatively lower capacity for the uptake of $CFSE^+$ donor cells at similar time points (Fig. 5A). This increased uptake of $CFSE^+$ donor cells by host $CD8\alpha^+$ $CD11c^+$ DCs is shown quantitatively in Fig. 5B. Collectively, these results suggest that the $CD8\alpha^+$ $CD11c^+$ $CD40^+$ DC population may aid in the rapid clearance of apoptotic cells following IFN-I-induced attrition and, in turn, become reactive with annexin V in the process.

Apoptosis of T cells during the early immune response to LCMV. Having established that the attrition of memory phenotype T cells, following poly(I:C) treatment, was due to apoptosis of CD4 and CD8 T cells in the wake of an increase in annexin V^+ $CD8\alpha^+$ DCs, we examined the attrition and apop-

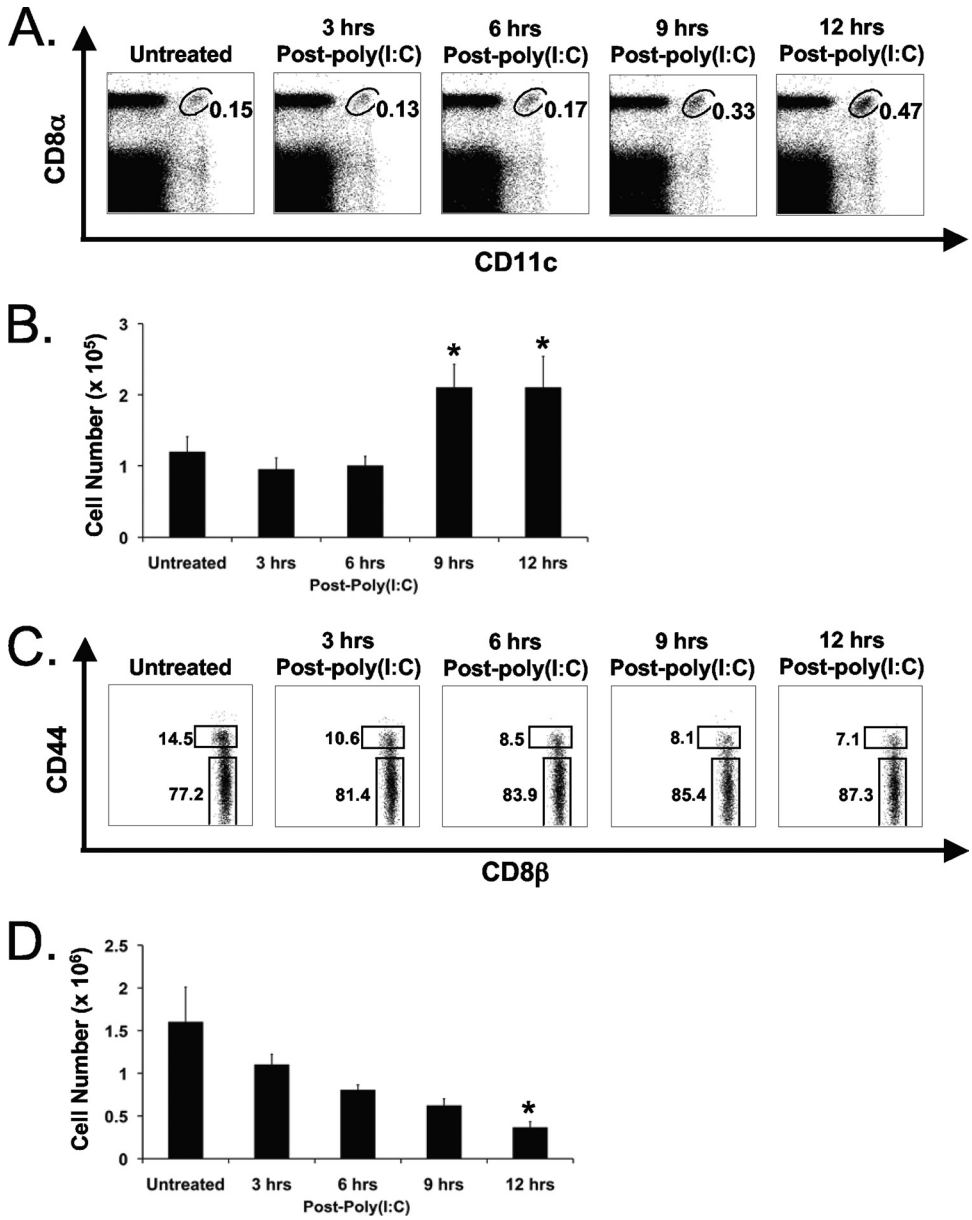

FIG. 2. The poly(I:C)-induced decrease in CD8β$^+$ CD44^{high} T cells correlates with an increase in CD8α$^+$ DCs. C57BL/6 mice were inoculated with poly(I:C) i.p. Splenocytes were harvested at 0 (untreated), 3, 6, 9, and 12 h after poly(I:C) inoculation. (A) Percentage of CD8α$^+$ DCs at multiple time points following poly(I:C) treatment. (B) Absolute numbers of CD8α$^+$ CD11c$^+$ DCs at multiple time points following poly(I:C) treatment. *, $P < 0.05$ relative to untreated mice. Error bars indicate standard deviations. (C) Percentage of CD8β$^+$ CD44$^{high/low}$ T cells at multiple time points following poly(I:C) treatment. (D) Absolute numbers of CD8β$^+$ CD44^{high} T cells at multiple time points following poly(I:C) treatment. Gates were set on 7-AAD$^-$ cells. Absolute numbers were based upon percentages obtained via flow cytometry. *, $P < 0.05$ relative to untreated mice. The data are representative of three independent experiments with three mice per group.

tosis of these populations in mice infected with LCMV. Figure 6A shows an increase in annexin V-reactive CD8α$^+$ DCs in the spleen early after LCMV infection (days 0 to 2). This population declined thereafter (29). This increase in CD8α$^+$ DCs was not as dramatic as with poly(I:C), but these DCs, like those induced by poly(I:C), expressed CD40 (Fig. 6A, quadrant 3, inset). A slight increase in the percentage of annexin V-reactive CD8α and CD8β T cells was observed at early time points following LCMV infection (Fig. 6A, quadrant 1), but this increase was very modest. Therefore, we reevaluated the apoptotic properties of CD44^{high} T cells at the early stages of infection with LCMV using a CD8β MAb, as no DCs were detected in the CD8β$^+$ CD44^{high} gate (Fig. 6A). There was a substantial decrease in CD8β$^+$ CD44^{high} T cell numbers as early as day 2 postinfection (Fig. 6B), and this correlated with an increase in caspase 3 activation detected *ex vivo* and peaking at day 3, though again, annexin V staining, which also peaked on day 3, was relatively low (Fig. 6C). DNA fragmentation, as visualized by TUNEL after a 5-h incubation in culture, was substantial and also peaked at day 3 (Fig. 6D). At day 4 postin-

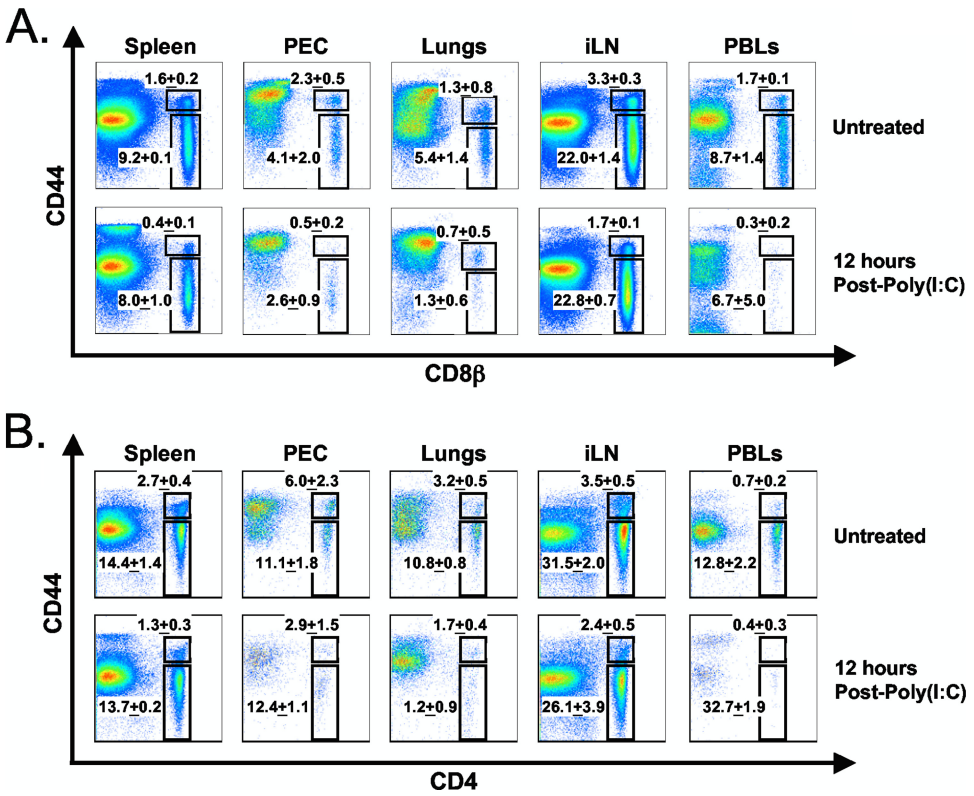

FIG. 3. Trafficking to other compartments does not account for the loss of CD8β$^+$ CD44^{high} and CD4$^+$ CD44^{high} T cells from the spleen following poly(I:C) treatment. C57BL/6 mice were inoculated with poly(I:C) i.p. Splenocytes, peritoneal exudate cells (PECs), lungs, inguinal lymph nodes (iLN), and peripheral blood lymphocytes (PBLs) were harvested at 0 (untreated) and 12 h postinoculation. (A) Plots display the percentages of untreated and poly(I:C)-treated CD8β$^+$ CD44$^{high/low}$ T cells. (B) Plots display the percentages of untreated and poly(I:C)-treated CD4$^+$ CD44$^{high/low}$ T cells. Gates were set upon 7-AAD$^-$ cells. Each plot is representative of three mice per group, and the percentages displayed on each plot are the averages for three mice per group. The data are representative of two independent experiments, each with three mice per group.

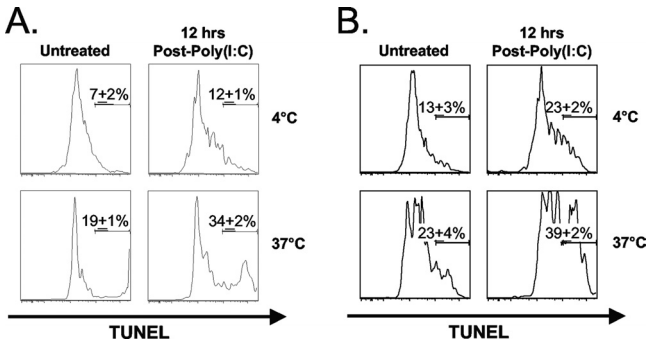

FIG. 4. The poly(I:C)-induced attrition of CD8β$^+$ CD44^{high} and CD4$^+$ CD44^{high} T cells correlates with an increase in DNA fragmentation. C57BL/6 mice were inoculated with poly(I:C) i.p. Splenocytes were harvested at 0 (untreated) and 12 h after poly(I:C) treatment. DNA fragmentation was assessed via TUNEL staining after a brief *in vitro* culture of splenocytes for 5 h at either 37°C or 4°C (see Materials and Methods). (A) Plots show the percentage of untreated or poly(I:C)-treated TUNEL$^+$ CD8β$^+$ CD44^{high} T cells (37°C and 4°C). (B) Plots show the percentage of untreated or poly(I:C)-treated TUNEL$^+$ CD4$^+$ CD44^{high} T cells (37°C and 4°C). Each plot is representative of three mice per group, while the percentages displayed on each plot are the averages for three mice per group. The data are representative of three independent experiments.

fection, CD8β$^+$ CD44^{high} T cell numbers began to recover (Fig. 6B), correlating with a decrease in caspase 3 activation (Fig. 6B) and DNA fragmentation (Fig. 6D). It should be noted that highly defined antigen-specific T cells can easily be stained *ex vivo* with annexin V at later stages of an LCMV infection (days 7 to 12), when the clearance system for apoptotic cells is likely overwhelmed (40). Nevertheless, these data show that much of the early loss of memory phenotype T cells following LCMV infection is due to an apoptotic mechanism.

Factors associated with the virus-induced apoptosis of memory T cells. While the loss of CD8β$^+$ CD44^{high} T cells is IFN-I dependent, the molecules downstream of IFN-I signaling that may contribute to this loss are currently undefined. Having established that the LCMV-induced loss of CD8β$^+$ CD44^{high} T cells was at least partly due to apoptosis, we next evaluated the mechanisms that may contribute to this loss. Bim is a proapoptotic molecule involved in mitochondrion-induced apoptosis, and IFN-I was found to induce apoptosis in certain myeloma cell lines through the upregulation of Bim (15). Bim has been shown to play a role in inhibiting the decline in number of LCMV-specific T cells at the termination of infection and to influence the specificity of clonal exhaustion during persistent LCMV infections (16, 44). We questioned whether the early apoptosis of CD8β$^+$ CD44^{high} T cells would be re-

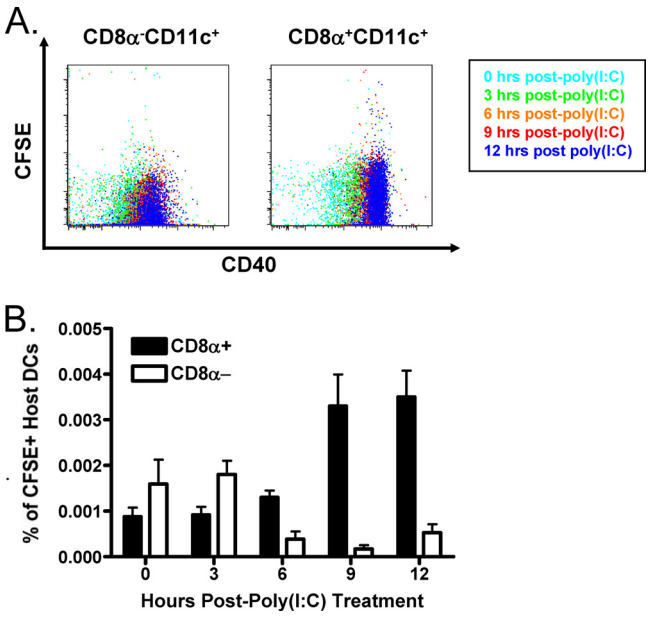

FIG. 5. The poly(I:C)-induced increase in CD8α$^+$ DCs may contribute to the rapid clearance of apoptotic cells. A total of 2×10^7 CFSE-labeled wild-type splenocytes (Ly5.1) were adoptively transferred into congenic wild-type recipients (Ly5.2). Splenocytes were harvested at 0 (untreated), 3, 6, 9, and 12 h after poly(I:C) treatment. (A) The capacities of Ly5.2$^+$ CD8α$^+$ CD11c$^+$ and Ly5.2$^+$ CD8α$^-$ CD11c$^+$ DCs to take up Ly5.1$^+$ CFSE$^+$ cells were correlated with CD40 expression at indicated the time points Doublets were excluded via pulse width, and gates were set upon Ly5.2$^+$ CD11c$^+$ 7-AAD$^-$ cells. (B) The plot shows the percentages of host (Ly5.2) CD8α$^+$ and CD8α$^-$ CFSE$^+$ DC populations following poly(I:C) treatment. Each data point is the average for three mice, and the data are representative of three independent experiments, each with three mice per data point. Error bars indicate standard deviations.

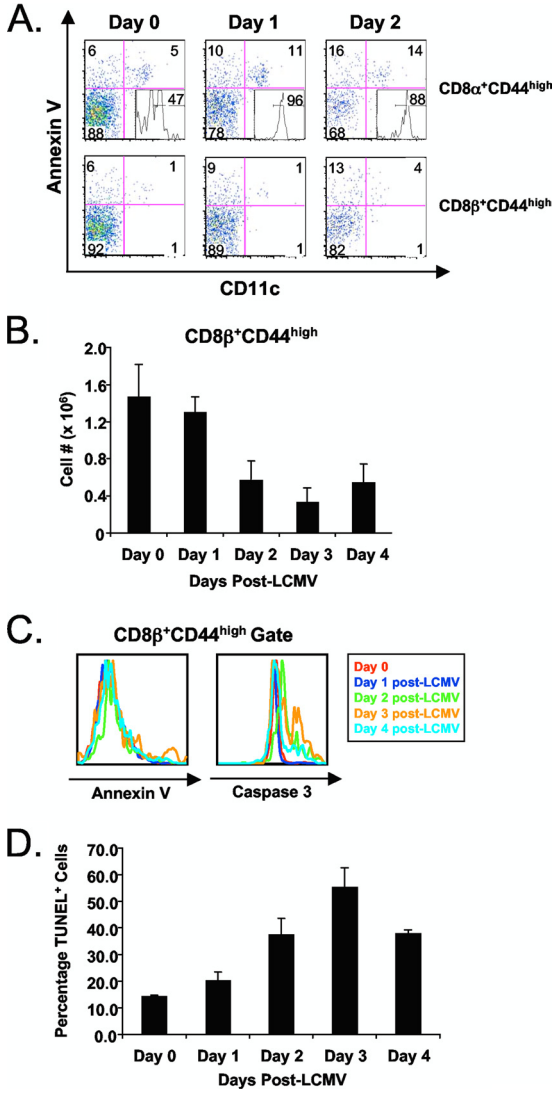

FIG. 6. The LCMV-induced attrition of CD8β$^+$ CD44^{high} T cells correlates with a substantial increase in DNA fragmentation and caspase 3 activation but not annexin V reactivity. C57BL/6 mice were infection with LCMV-Armstrong i.p. Splenocytes were harvested at 0, 1, 2, 3, and 4 days postinfection. DNA fragmentation was assessed via TUNEL staining after a brief *in vitro* culture of splenocytes for 5 h at 37°C (see Materials and Methods). (A) Annexin V and CD11c staining on CD8α$^+$ CD44^{high} and CD8β$^+$ CD44^{high} cells at days 0,1, and 2 after LCMV infection. Histogram inset in quadrant 3 show CD40 expression on the annexin V$^+$ CD11c$^+$ CD8α$^+$ CD44^{high} population (quadrant 2). (B) Absolute CD8β$^+$ CD44^{high} T cell numbers at 0, 1, 2, 3, and 4 days postinfection. Error bars indicate standard deviations. (C) Histogram overlays depicting CD8β$^+$ CD44^{high} annexin V reactivity and caspase 3 activation on days 0, 1, 2, 3, and 4 after LCMV infection. Line color corresponds to day after LCMV infection. (D) Percentages of TUNEL$^+$ CD8β$^+$ CD44^{high} T cells isolated from mice at days 0, 1, 2, 3, and 4 postinfection. Absolute numbers were based upon percentages obtained via flow cytometry. The data are representative of three independent experiments with three mice per group.

duced in Bim KO mice relative to wild-type mice at 3 days after LCMV infection. The cell numbers among individual Bim KO mice were quite variable, making studies on total cell numbers difficult to address without using very large numbers of mice for replicas. Nevertheless, Fig. 7A shows a representative experiment where about 50% of wild-type CD8β$^+$ CD44^{high} T cells were depleted in percentage at 3 days after LCMV infection, compared to fewer than 30% of Bim KO CD8β$^+$ CD44^{high} cells, relative to their respective untreated controls (Fig. 7A).

Since the variations in cell numbers among Bim KO mice were problematic for these analyses, we rationalized that the degree of apoptosis within individual mice was a more reliable indicator of whether Bim was influencing LCMV-induced apoptosis of CD8β$^+$ CD44^{high} T cells. Therefore, we tested these cells in the TUNEL assay after *in vitro* incubation at 37°C. At 3 days after LCMV infection, the percentage of Bim KO TUNEL$^+$ CD8β$^+$ CD44^{high} T cells was significantly lower than in the wild type ($n = 3$; $P < 0.05$) (Fig. 7B). Interestingly, untreated Bim KO mice had a higher percentage of effector memory phenotype CD8 T cells (CCR7$^-$ CD62L$^-$) than wild-type controls (data not shown), and others have shown that effector memory phenotype CD8 T cells are less susceptible to IFN-I-induced attrition than central memory CD8 T cells (20).

Given that the attrition of memory T cells is linked to the action of type I IFNs, we questioned whether the Bim KO mice generated normal levels of IFN-I. Sera from wild-type and Bim KO mice, at 12 h after poly(I:C) treatment or 3 days after LCMV infection, had similar type I IFN endpoint dilution

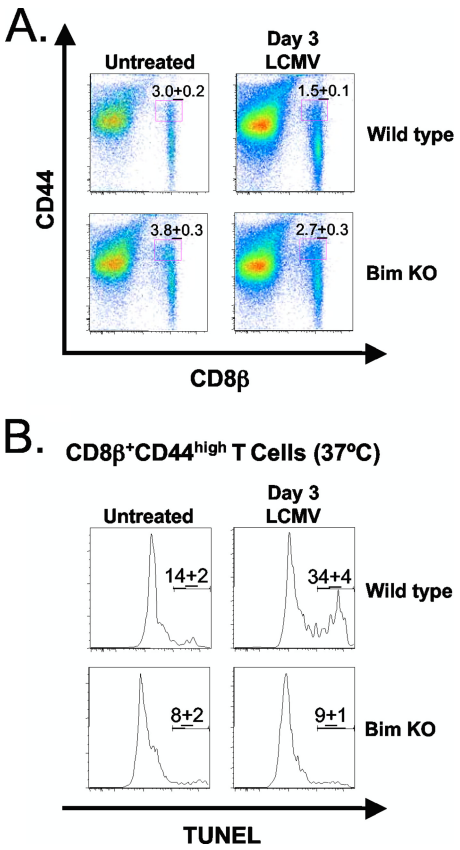

FIG. 7. The LCMV-induced apoptosis of CD8β$^+$ CD44^{high} T cells is partially dependent on Bim. C57BL/6 (wild-type) and Bim-deficient (Bim KO) mice were infected with LCMV-Armstrong i.p. Splenocytes were harvested at day 0 (untreated) and 3 days postinfection. DNA fragmentation was assessed via TUNEL staining after a brief *in vitro* culture of splenocytes for 5 h at 37°C (see Materials and Methods). (A) The plots show the percentages of untreated and LCMV-infected wild-type and Bim KO CD8β$^+$ CD44^{high} T cells. (B) The plots show the percentages of untreated and LCMV-infected wild-type and Bim KO TUNEL$^+$ CD8β$^+$ CD44^{high} T cells. Each plot is representative of three mice per group, while the percentages are the averages for three mice per group. The data are representative of three independent experiments.

titers in a standard bioassay using microtiter plate wells of L-929 cells challenged with vesicular stomatitis virus (~1/2,500 dilution of serum). Therefore, differences in apoptosis between wild-type and Bim KO T cells cannot be attributed to differences in IFN-I production.

Reduced attrition of cross-reactive memory cells in old LCMV-immune mice may limit the diversity of the ensuing immune response to heterologous Pichinde virus infection. Others have shown that aged mice develop less memory T cell attrition and mount a weaker CD8 T cell response to LCMV than do younger mice (19, 23). LCMV and PV encode epitopes in the nucleoprotein NP205-212 sharing 6 of 8 amino acids. In a naïve host, NP205 is normally a subdominant epitope for both viruses, specific for usually <3% of the CD8 T cells, However, due to a selective expansion of NP205-specific cross-reactive memory CD8 T cells, the NP205-specific T cell response becomes more dominant when LCMV-immune mice are infected with PV, demonstrating how cross-reactive expansion of T cells can alter the hierarchy of T cell responses (8). Using this LCMV/PV cross-reactive model, we questioned whether the reduced apoptosis of a cross-reactive memory CD8 population (NP205) in aged LCMV-immune mice would allow the cross-reactive cells to more vigorously dominate the immune response following heterologous PV challenge, as we previously predicted by computer modeling (3). These computer models predicted that attrition of cross-reactive memory CD8 T cells reduces their immunodominance and allows for a more diverse immune response, because memory CD8 T cells are more susceptible to the IFN-I-induced attrition than are naïve CD8 T cells (3, 27).

We therefore tested the hypothesis that aged mice, which have less IFN-I-induced attrition than young mice, would mount a greater cross-reactive response than would young mice. Young and aged naïve (Fig. 8A) or LCMV-immune (Fig. 8B and C) mice were infected with PV, which, like LCMV, induces a potent IFN-I response. At day 8 postinfection, the frequencies of the cross-reactive memory (NP205) and non-cross-reactive normally immunodominant PV-specific (NP38) CD8 T cells were determined via intracellular IFN-γ assay. Both young and aged naïve controls had comparable PV NP38-specific responses at day 8 postinfection (18% and 16% of the CD8 population, respectively) (Fig. 8A); NP205 responses were <1% in these mice. Figure 8B shows that at day 8 postinfection, a representative LCMV-immune young mouse had an NP205-to-NP38 ratio of under 1, suggesting that the loss of the cross-reactive, NP205-specific memory CD8 population allowed for the successful expansion of the newly arising NP38-specific response. A representative aged LCMV-immune mouse had an NP205-to-NP38 ratio of over 1, suggesting that the lack of cross-reactive, NP205-specific memory CD8 cell attrition allowed this population to dominate, thereby, hindering the expansion of the newly arising NP38 response (Fig. 8B). This point is further emphasized in Fig. 8C, where the NP205-to-NP38 ratios in multiple young and old LCMV-immune mice were compared at day 8 after PV infection. This revealed young mice to have a significantly lower ratio than aged mice (1.5 versus 2.5, respectively) (Fig. 8C) ($P < 0.05$). This difference in ratio could be due to aged LCMV-immune mice having higher NP205 frequencies prior to PV infection. Therefore, the potential for the NP205 population to dominate may be dependent upon the initial NP205 frequency prior to infection. However, there was no correlation between the initial NP205 frequency and its ability to dominate the immune response at day 8 after PV infection (as indicated by the NP205/NP38 ratio) when data from both young and aged mice were pooled ($r^2 = 0.1936$; $n = 14$) or analyzed separately (young, $r^2 = 0.1850$ [$n = 7$]; aged, $r^2 = 0.3280$ [$n = 7$]). Although there could be other interpretations, these results are consistent with the concept that the early virus-induced attrition limits the size of the cross-reactive memory pool (NP205) and allows for the successful expansion of non-cross-reactive clones from the naïve pool.

DISCUSSION

It was previously shown that the IFN-I-induced attrition of CD8α$^+$ CD44^{high} cells occurring after viral infection or TLR agonist treatment correlated with an increase in annexin V

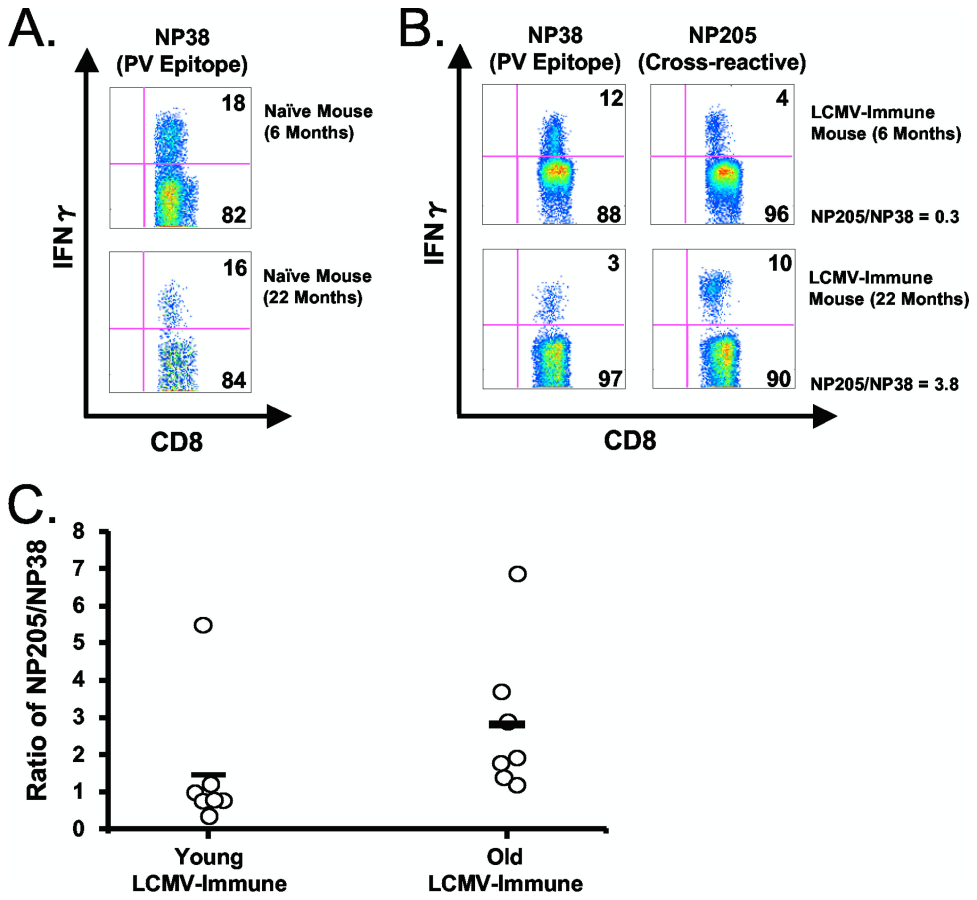

FIG. 8. Reduced attrition in aged LCMV-immune mice limits the diversity in the arising T cell response following heterologous Pichinde virus (PV) challenge. Young (6 to 8 months) and aged (18 to 22 months) LCMV-immune mice were prebled to determine NP205-specific $CD8^+$ T cell frequencies prior to infection with PV, via an intracellular cytokine assay. Mice were rebled on day 8 after PV infection, and the ratios of the NP205 to the NP38 response were determined via intracellular cytokine assay. (A) Frequencies of NP38-specific $CD8^+$ T cells, as revealed by intracellular IFN-γ assay, in young and aged naïve mice. (B) Frequencies of NP38- and NP205-specific $CD8^+$ T cells at day 8 after PV infection, as revealed by intracellular IFN-γ assay, in young and old LCMV-immune mice. (C) Ratio of the NP205 to NP38 response for multiple young and old LCMV-immune mice (day 8 after PV infection). The plots in panels A and B show one representative mouse, while panel C shows the NP205/NP38 frequencies for all mice over multiple experiments.

reactivity, suggesting that this loss occurred through an apoptotic mechanism (Fig. 1) (3, 27). It was believed that this $CD8\alpha^+$ $CD44^{high}$ population consisted primarily of T cells, but here we show that a population of "lymphoid" $CD8\alpha^+$ DCs, within the $CD8\alpha^+$ $CD44^{high}$ gate, increased substantially upon poly(I:C) treatment (Fig. 1). This DC population accounted for the annexin V-reactive cells at 12 h following poly(I:C) treatment (Fig. 1). This observation made necessary a reevaluation of the IFN-I-induced attrition of memory T cells occurring during viral infection or poly(I:C) treatment. Our results using anti-CD8β antibody, which is a more exclusive stain for $CD8^+$ T cells than an anti-CD8α antibody, indicated that there was even more CD8 T cell attrition than previously thought (Fig. 2C and D) and that there also was substantial attrition of $CD4^+$ memory phenotype T cells.

Three potential mechanisms that could account for this loss were migration away from the organ tested (spleen), increased adherence to structural tissue, and death. Although inflammatory cytokines can alter the trafficking patterns of T cells, we observed a similar loss of $CD8\beta^+$ $CD44^{high}$ and $CD4^+$ $CD44^{high}$ T cells in spleen, PECs, lungs, iLN, and peripheral blood following poly(I:C) treatment (Fig. 3A and B). A similar loss was also observed in the bone marrow (data not shown). Although it is difficult to rule out trafficking into compartments that we have not yet examined, these data indicate that the loss of $CD8\beta^+$ $CD44^{high}$ and $CD4^+$ $CD44^{high}$ T cells is a global phenomenon affecting many tissues, without an accumulation of cells at a discrete site of infection. Inflammatory cytokines can also affect the adherence properties of T cells. Others have reported a transient decline of antigen-specific memory CD8 T cells in the spleens of mice early after *Listeria monocytogenes* infection. One study suggests that this is due to a generalized IFN-I-dependent apoptosis (27), and another study concludes that this was a consequence of the T cells undergoing an antigen-presenting cell (APC)-dependent conditioning phase that renders them undetectable by flow cytometry but readily detectable by histological techniques (18). This phenomenon, termed T cell conditioning, is a process whereby APCs laden with antigen form aggregates with antigen-specific T cells, thereby preventing them from being properly extracted or pro-

cessed for analysis by flow cytometry (18, 26). However, the IFN-I-induced attrition affects all memory cells equally, whereas conditioning is antigen specific. LCMV infection causes substantial reductions in the frequencies of CD8 T cells that are specific to a heterologous virus as early as 2 days postinfection, and these frequencies do not recover as the infection resolves, a finding that neither migration nor T cell conditioning can account for (24). Further, we were unable to account for the T cell loss by treating tissues with Liberase (Roche), a purified enzyme blend (data not shown). This suggests that long-term loss in memory is, in large part, a consequence of the IFN-I-dependent apoptotic loss in memory CD8 T cells.

Here we demonstrate substantial levels of apoptosis of memory phenotype CD8 and CD4 T cells when T cells isolated from poly(I:C)-treated or LCMV-infected mice are examined by TUNEL assay after a short *in vitro* incubation. This apoptosis could be readily seen only if cells from affected mice were incubated *in vitro* for 4 to 5 h, as the *in vivo* clearance system for apoptotic cells seems to be quite effective at the time points studied. Here we also report the first evidence of Bim's involvement in the early apoptosis of T cells following LCMV infection. The attrition of $CD8\beta^+$ $CD44^{high}$ T cells was reduced in Bim KO mice at 3 days after LCMV infection relative to that in wild-type mice (Fig. 7A). The reduced attrition corresponded with a decrease in DNA fragmentation, as revealed by TUNEL, in Bim KO $CD8\beta^+$ $CD44^{high}$ T cells relative to wild-type $CD8\beta^+$ $CD44^{high}$ T cells (Fig. 7B). Overall, the reduced attrition coupled with the reduction in DNA fragmentation in Bim KO mice suggests that Bim may contribute to the apoptosis of $CD8\beta^+$ $CD44^{high}$ T cells following LCMV infection, and these results are another argument supporting the concept that apoptosis is indeed responsible for memory T cell attrition. Nevertheless, Bim KO mice infected with LCMV were not completely resistant to the early attrition (Fig. 7A), suggesting that additional mechanisms might be involved.

Type I IFN has been shown to cause the attrition of certain myeloma cell lines through a mitochondrion-induced pathway involving Bim (11, 32). As mentioned above, serum IFN-I levels were similar in wild-type and Bim KO mice at 3 days after LCMV infection. Therefore, the reduced attrition in Bim KO mice infected with LCMV is not due to lower levels of type I IFN induction.

It is unclear whether IFN-I exerts its effects on T cell attrition directly or indirectly. Recently, we generated IFN-I-R KO/wild-type bone marrow chimeric mice and found that the IFN-I-R KO memory phenotype T cell population underwent less attrition following LCMV-Armstrong infection (day 3) or poly(I:C) treatment (12 h), relative to the corresponding wild-type population. These data suggest that IFN-I may exert at least some of its effects directly, which is consistent with IFN-I modulating Bim expression levels. We document a type I IFN-dependent increase in $CD8\alpha^+$ DCs that was greater following poly(I:C) treatment (Fig. 1 and 2) than after LCMV infection (Fig. 6A). This is not surprising since $CD8\alpha^+$ DCs can also be activated through TLR3, a receptor for poly(I:C) (34). Interestingly, this increase in $CD8\alpha^+$ DCs correlated with the decrease in the $CD8\beta^+$ $CD44^{high}$ T cells (Fig. 2). $CD8\alpha^+$ DCs might aid in the rapid clearance of apoptotic cells following poly(I:C) treatment *in vivo*, as there was an increase in the uptake of CFSE from labeled congenic donor cells by host $CD8\alpha^+$ DCs, following poly(I:C) treatment (Fig. 5). Others have shown that the engulfment of apoptotic cells results in an increase in class II expression, a result consistent with our finding of increased class II expression at 12 h after poly(I:C) treatment (Fig. 1E) (12). T cells and DCs are in close contact during antigen presentation, but this would not explain the increased uptake of CFSE from labeled donor cells by host DCs, since doublets were gated out using pulse width prior to analysis.

Monocytes have been shown to phagocytose apoptotic bodies that are shed from the neighboring apoptotic cell and, in the process, can become "false positive" by the annexin V assay (25). This suggests that $CD8\alpha^+$ DCs might become annexin V^+ upon engulfing apoptotic lymphocytes. The apoptotic phenotype, as indicated by an increase in annexin V reactivity, suggests that the plasma membrane of the $CD8\alpha^+$ DC might fuse with the plasma membrane of the apoptotic body it engulfs. Phagocytic cells expressing T cell immunoglobulin- and mucin-domain-containing molecule (Tim4) have been shown to associate with exosomes carrying exposed phosphatidylserine, which may also account for the observed increase in annexin V reactivity (28). Nevertheless, the increased annexin V reactivity also suggests that the DCs could actually be dying. The typical life span of mature DCs is estimated to be 3 days *in vivo* (17, 22). Also, DC populations decline in number by day 3 postinfection. It is not known whether this drop in DCs is due to migration, phenotypic alterations, and/or cell death, but it is known to be type I IFN dependent (29). It has been shown that the surface expression of phosphatidylserine on macrophages is required for phagocytosis of apoptotic lymphocytes. Pretreating these macrophages with annexin V was found to inhibit phagocytosis of apoptotic thymocytes (9). Interestingly, our apoptosis PCR array analysis revealed an increase in IL-10 RNA in the $CD8\alpha^+$ $CD44^{high}$ population, containing $CD8\alpha^+$ DCs, at 6 h after poly(I:C) treatment. Exposure of DCs to IL-10 can suppress the induction of antiapoptotic genes, coinciding with the spontaneous apoptosis of the DC (10).

Our computer modeling predicted that if cross-reactive antigen prevents the type I IFN-induced deletion of a memory T cell population, those cross-reactive memory T cells would compete against a more diverse and higher-affinity new T cell response to the newly encountered pathogen (3). Creating a biological model to study the consequence of the lack of type I IFN-induced attrition of memory CD8 T cells during the early immune response had proven problematic, in part, because it is difficult to separate the T cell apoptosis-inducing properties of IFN-I from the myriad of other IFN-I-induced events that regulate antigen presentation and the subsequent immune response. Nevertheless, we took advantage of the finding that aged mice develop less attrition than younger mice (19, 20) and questioned whether the reduced apoptosis of the cross-reactive memory CD8 population (NP205) in aged LCMV-immune mice, following heterologous virus (PV) challenge, would allow them to dominate the immune response. We show in Fig. 8 that the cross-reactive memory CD8 T cell response (NP205) was more immunodominating in aged LCMV-immune mice than in younger LCMV-immune mice at day 8 after PV challenge (Fig. 8B and C). The diminished PV response in aged LCMV-immune mice relative to younger

LCMV-immune mice could be attributed to aged mice having a smaller immunologically naïve repertoire, but both young and old naïve mice mounted similar PV-specific responses at day 8 postinfection (Fig. 8A). These results may indicate that the impact of heterologous immunity, whether it be beneficial or detrimental, may be more profound in older individuals due to the enhanced responses of cross-reactive T cells.

ACKNOWLEDGMENTS

This work was supported by U.S. National Institutes of Health research grants AI017672, AI081675, AI073871, AI46692, AI054455, CA65861, NS054948, and DK080665. R.J.D. is an investigator of the Howard Hughes Medical Institute.

The opinions expressed are those of the authors and not necessarily those of the NIH.

We thank Varun Kapoor for helpful discussions.

REFERENCES

1. **Albert, M. L., S. F. Pearce, L. M. Francisco, B. Sauter, P. Roy, R. L. Silverstein, and N. Bhardwaj.** 1998. Immature dendritic cells phagocytose apoptotic cells via alphavbeta5 and CD36, and cross-present antigens to cytotoxic T lymphocytes. J. Exp. Med. **188:**1359–1368.
2. **Albert, M. L., B. Sauter, and N. Bhardwaj.** 1998. Dendritic cells acquire antigen from apoptotic cells and induce class I-restricted CTLs. Nature **392:**86–89.
3. **Bahl, K., S. K. Kim, C. Calcagno, D. Ghersi, R. Puzone, F. Celada, L. K. Selin, and R. M. Welsh.** 2006. IFN-induced attrition of CD8 T cells in the presence or absence of cognate antigen during the early stages of viral infections. J. Immunol. **176:**4284–4295.
4. **Baize, S., P. Marianneau, P. Loth, S. Reynard, A. Journeaux, M. Chevallier, N. Tordo, V. Deubel, and H. Contamin.** 2009. Early and strong immune responses are associated with control of viral replication and recovery in Lassa virus-infected cynomolgus monkeys. J. Virol. **83:**5890–5903.
5. **Banchereau, J., F. Bazan, D. Blanchard, F. Briere, J. P. Galizzi, C. van Kooten, Y. J. Liu, F. Rousset, and S. Saeland.** 1994. The CD40 antigen and its ligand. Annu. Rev. Immunol. **12:**881–922.
6. **Bouillet, P., D. Metcalf, D. C. Huang, D. M. Tarlinton, T. W. Kay, F. Kontgen, J. M. Adams, and A. Strasser.** 1999. Proapoptotic Bcl-2 relative Bim required for certain apoptotic responses, leukocyte homeostasis, and to preclude autoimmunity. Science **286:**1735–1738.
7. **Bourgeois, C., B. Rocha, and C. Tanchot.** 2002. A role for CD40 expression on CD8+ T cells in the generation of CD8+ T cell memory. Science **297:**2060–2063.
8. **Brehm, M. A., A. K. Pinto, K. A. Daniels, J. P. Schneck, R. M. Welsh, and L. K. Selin.** 2002. T cell immunodominance and maintenance of memory regulated by unexpectedly cross-reactive pathogens. Nat. Immunol. **3:**627–634.
9. **Callahan, M. K., P. Williamson, and R. A. Schlegel.** 2000. Surface expression of phosphatidylserine on macrophages is required for phagocytosis of apoptotic thymocytes. Cell Death Differ. **7:**645–653.
10. **Chang, W. L., N. Baumgarth, M. K. Eberhardt, C. Y. Lee, C. A. Baron, J. P. Gregg, and P. A. Barry.** 2007. Exposure of myeloid dendritic cells to exogenous or endogenous IL-10 during maturation determines their longevity. J. Immunol. **178:**7794–7804.
11. **Chen, Q., B. Gong, A. S. Mahmoud-Ahmed, A. Zhou, E. D. Hsi, M. Hussein, and A. Almasan.** 2001. Apo2L/TRAIL and Bcl-2-related proteins regulate type I interferon-induced apoptosis in multiple myeloma. Blood **98:**2183–2192.
12. **Clayton, A. R., R. L. Prue, L. Harper, M. T. Drayson, and C. O. Savage.** 2003. Dendritic cell uptake of human apoptotic and necrotic neutrophils inhibits CD40, CD80, and CD86 expression and reduces allogeneic T cell responses: relevance to systemic vasculitis. Arthritis Rheum. **48:**2362–2374.
13. **Cunha, B. A., B. P. McDermott, and S. S. Mohan.** 2004. Prognostic importance of lymphopenia in West Nile encephalitis. Am. J. Med. **117:**710–711.
14. **Geisbert, T. W., L. E. Hensley, T. R. Gibb, K. E. Steele, N. K. Jaax, and P. B. Jahrling.** 2000. Apoptosis induced in vitro and in vivo during infection by Ebola and Marburg viruses. Lab. Invest. **80:**171–186.
15. **Gomez-Benito, M., P. Balsas, X. Carvajal-Vergara, A. Pandiella, A. Anel, I. Marzo, and J. Naval.** 2007. Mechanism of apoptosis induced by IFN-alpha in human myeloma cells: role of Jak1 and Bim and potentiation by rapamycin. Cell Signal. **19:**844–854.
16. **Grayson, J. M., A. E. Weant, B. C. Holbrook, and D. Hildeman.** 2006. Role of Bim in regulating CD8+ T-cell responses during chronic viral infection. J. Virol. **80:**8627–8638.
17. **Ingulli, E., A. Mondino, A. Khoruts, and M. K. Jenkins.** 1997. In vivo detection of dendritic cell antigen presentation to CD4(+) T cells. J. Exp. Med. **185:**2133–2141.
18. **Jabbari, A., K. L. Legge, and J. T. Harty.** 2006. T cell conditioning explains early disappearance of the memory CD8 T cell response to infection. J. Immunol. **177:**3012–3018.
19. **Jiang, J., F. Anaraki, K. J. Blank, and D. M. Murasko.** 2003. T cells from aged mice are resistant to depletion early during virus infection. J. Immunol. **171:**3353–3357.
20. **Jiang, J., D. Gross, S. Nogusa, P. Elbaum, and D. M. Murasko.** 2005. Depletion of T cells by type I interferon: differences between young and aged mice. J. Immunol. **175:**1820–1826.
21. **Jiang, J., L. L. Lau, and H. Shen.** 2003. Selective depletion of nonspecific T cells during the early stage of immune responses to infection. J. Immunol. **171:**4352–4358.
22. **Kamath, A. T., J. Pooley, M. A. O'Keeffe, D. Vremec, Y. Zhan, A. M. Lew, A. D'Amico, L. Wu, D. F. Tough, and K. Shortman.** 2000. The development, maturation, and turnover rate of mouse spleen dendritic cell populations. J. Immunol. **165:**6762–6770.
23. **Kapasi, Z. F., K. Murali-Krishna, M. L. McRae, and R. Ahmed.** 2002. Defective generation but normal maintenance of memory T cells in old mice. Eur. J. Immunol. **32:**1567–1573.
24. **Kim, S. K., and R. M. Welsh.** 2004. Comprehensive early and lasting loss of memory CD8 T cells and functional memory during acute and persistent viral infections. J. Immunol. **172:**3139–3150.
25. **Marguet, D., M. F. Luciani, A. Moynault, P. Williamson, and G. Chimini.** 1999. Engulfment of apoptotic cells involves the redistribution of membrane phosphatidylserine on phagocyte and prey. Nat. Cell Biol. **1:**454–456.
26. **Maxwell, J. R., R. J. Rossi, S. J. McSorley, and A. T. Vella.** 2004. T cell clonal conditioning: a phase occurring early after antigen presentation but before clonal expansion is impacted by Toll-like receptor stimulation. J. Immunol. **172:**248–259.
27. **McNally, J. M., C. C. Zarozinski, M. Y. Lin, M. A. Brehm, H. D. Chen, and R. M. Welsh.** 2001. Attrition of bystander CD8 T cells during virus-induced T-cell and interferon responses. J. Virol. **75:**5965–5976.
28. **Miyanishi, M., K. Tada, M. Koike, Y. Uchiyama, T. Kitamura, and S. Nagata.** 2007. Identification of Tim4 as a phosphatidylserine receptor. Nature **450:**435–439.
29. **Montoya, M., M. J. Edwards, D. M. Reid, and P. Borrow.** 2005. Rapid activation of spleen dendritic cell subsets following lymphocytic choriomenigitis virus infection of mice: analysis of the involvement of type 1 IFN. J. Immunol. **174:**1851–1861.
30. **Nabeshima, S., M. Murata, K. Kikuchi, H. Ikematsu, S. Kashiwagi, and J. Hayashi.** 2002. A reduction in the number of peripheral CD28+CD8+T cells in the acute phase of influenza. Clin. Exp. Immunol. **128:**339–346.
31. **Nishimura, Y., T. Igarashi, A. Buckler-White, C. Buckler, H. Imamichi, R. M. Goeken, W. R. Lee, B. A. Lafont, R. Byrum, H. C. Lane, V. M. Hirsch, and M. A. Martin.** 2007. Loss of naive cells accompanies memory CD4+ T-cell depletion during long-term progression to AIDS in simian immunodeficiency virus-infected macaques. J. Virol. **81:**893–902.
32. **Otsuki, T., O. Yamada, H. Sakaguchi, A. Tomokuni, H. Wada, Y. Yawata, and A. Ueki.** 1998. Human myeloma cell apoptosis induced by interferon-alpha. Br. J. Haematol. **103:**518–529.
33. **Schneider-Schaulies, S., and J. Schneider-Schaulies.** 2009. Measles virus-induced immunosuppression. Curr. Top. Microbiol. Immunol. **330:**243–269.
34. **Schulz, O., S. S. Diebold, M. Chen, T. I. Naslund, M. A. Nolte, L. Alexopoulou, Y. T. Azuma, R. A. Flavell, P. Liljestrom, and C. Reis e Sousa.** 2005. Toll-like receptor 3 promotes cross-priming to virus-infected cells. Nature **433:**887–892.
35. **Tompkins, M. B., P. D. Nelson, R. V. English, and C. Novotney.** 1991. Early events in the immunopathogenesis of feline retrovirus infections. J. Am. Vet. Med. Assoc. **199:**1311–1315.
36. **van der Most, R. G., K. Murali-Krishna, J. L. Whitton, C. Oseroff, J. Alexander, S. Southwood, J. Sidney, R. W. Chesnut, A. Sette, and R. Ahmed.** 1998. Identification of Db- and Kb-restricted subdominant cytotoxic T-cell responses in lymphocytic choriomeningitis virus-infected mice. Virology **240:**158–167.
37. **van Engeland, M., L. J. Nieland, F. C. Ramaekers, B. Schutte, and C. P. Reutelingsperger.** 1998. Annexin V-affinity assay: a review on an apoptosis detection system based on phosphatidylserine exposure. Cytometry **31:**1–9.
38. **Varga, S. M., and R. M. Welsh.** 1998. Detection of a high frequency of virus-specific CD4+ T cells during acute infection with lymphocytic choriomeningitis virus. J. Immunol. **161:**3215–3218.
39. **Vremec, D., J. Pooley, H. Hochrein, L. Wu, and K. Shortman.** 2000. CD4 and CD8 expression by dendritic cell subtypes in mouse thymus and spleen. J. Immunol. **164:**2978–2986.
40. **Wang, X. Z., M. A. Brehm, and R. M. Welsh.** 2004. Preapoptotic phenotype of viral epitope-specific CD8 T cells precludes memory development and is an intrinsic property of the epitope. J. Immunol. **173:**5138–5147.
41. **Wang, X. Z., S. E. Stepp, M. A. Brehm, H. D. Chen, L. K. Selin, and R. M. Welsh.** 2003. Virus-specific CD8 T cells in peripheral tissues are more resistant to apoptosis than those in lymphoid organs. Immunity **18:**631–642.
42. **Welsh, R. M., Jr., P. W. Lampert, P. A. Burner, and M. B. Oldstone.** 1976. Antibody-complement interactions with purified lymphocytic choriomeningitis virus. Virology **73:**59–71.

43. **Whitton, J. L., P. J. Southern, and M. B. Oldstone.** 1988. Analyses of the cytotoxic T lymphocyte responses to glycoprotein and nucleoprotein components of lymphocytic choriomeningitis virus. Virology **162:**321–327.
44. **Wojciechowski, S., M. B. Jordan, Y. Zhu, J. White, A. J. Zajac, and D. A. Hildeman.** 2006. Bim mediates apoptosis of CD127(lo) effector T cells and limits T cell memory. Eur. J. Immunol. **36:**1694–1706.
45. **Wong, R. S., A. Wu, K. F. To, N. Lee, C. W. Lam, C. K. Wong, P. K. Chan, M. H. Ng, L. M. Yu, D. S. Hui, J. S. Tam, G. Cheng, and J. J. Sung.** 2003. Haematological manifestations in patients with severe acute respiratory syndrome: retrospective analysis. BMJ **326:**1358–1362.
46. **Yang, H. Y., P. L. Dundon, S. R. Nahill, and R. M. Welsh.** 1989. Virus-induced polyclonal cytotoxic T lymphocyte stimulation. J. Immunol. **142:**1710–1718.

JOURNAL OF VIROLOGY, June 2010, p. 6262 Vol. 84, No. 12
0022-538X/10/$12.00 doi:10.1128/JVI.00870-10

ERRATUM

Analysis of Apoptosis of Memory T Cells and Dendritic Cells during the Early Stages of Viral Infection or Exposure to Toll-Like Receptor Agonists

Kapil Bahl,[1] Anette Hübner,[3] Roger J. Davis,[3] and Raymond M. Welsh[2]*

Department of Pathology, Yale University School of Medicine, New Haven, Connecticut 06510[1]; Department of Pathology, Program in Immunology and Virology, University of Massachusetts Medical School, Worcester, Massachusetts 01655[2]; and Howard Hughes Medical Institute, University of Massachusetts Medical School, Worcester, Massachusetts 01605[3]

Volume 84, no. 10, p. 4866–4877, 2010. Page 4866: The byline should appear as shown above.